Applied Thermal Engineering 163 (2019) 114379

Contents lists available at ScienceDirect

Applied Thermal Engineering

journal homepage: www.elsevier.com/locate/apthermeng

High-efficiency solar steam generation based on blue brick-graphene inverted cone evaporator

Binglin Bai[a], Xiaohong Yang[a,b,*], Rui Tian[a,c,*], Wanchun Ren[a], Ru Suo[a], Haibo Wang[a]

[a] School of Energy and Power Engineering, Inner Mongolia University of Technology, Hohhot, Inner Mongolia 010051, China
[b] Key Laboratory of Wind and Solar Energy Utilization Technology, Ministry of Education, China
[c] Inner Mongolia Key Laboratory of Renewable Energy, China

HIGHLIGHTS

- A bi-layer inverted cone structure was prepared by daubing graphene on blue bricks.
- With the increase of graphene concentration, the evaporation rate of the system increases rapidly.
- The evaporation efficiency of the inverted cone structure is superior to the plane structure.
- As a traditional building material, BBG is an excellent evaporator for the development of solar steam generation.

GRAPHICAL ABSTRACT

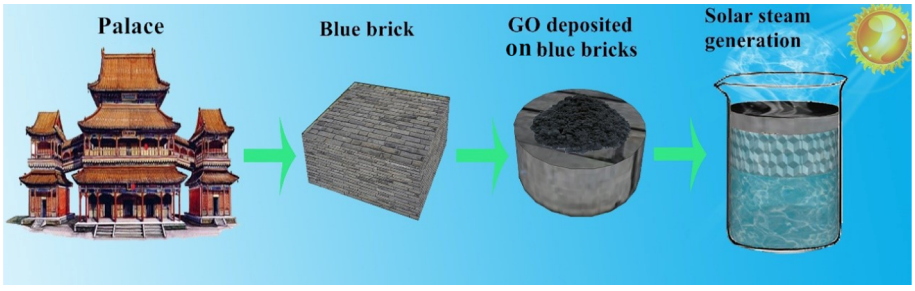

ARTICLE INFO

Keywords:
Solar energy
Blue brick
Steam generation
Light-heat conversion
Desalination

ABSTRACT

Solar steam generation, as a novel technology, has attracted received extensive attention in recent years. In order to further improve the evaporation performance of the solar steam generation system. In this work, a bi-layer inverted cone structure was prepared by daubing graphene on blue bricks for efficient solar steam generation. The excellent light-heat properties of the blue brick were characterized. The effects of system performance with different graphene concentrations were investigated. With the increase of graphene concentration, the evaporation rate of the system increases rapidly, and then gradually stabilizes at 1.09 kg m^{-2} h^{-1}. At the same time, a 3D inverted cone composite structure is designed. The optical absorption efficiency could reach 97.3% by light is intercepted by diffuse reflection, and the evaporation area is also increased, the evaporation rate is increased by 0.12 kg m^{-2} h^{-1}. Compared with the evaporation efficiency of plane structure, 90° inverted cone structure increased by about 8%. In addition, the blue brick-graphene shows an excellent water purification capacity, all four primary ions concentrations after purification are significantly reduced and the ion rejection ratios of four primary ions are close to 99.8%. Hence, we conclude that this work could provide a new method for high-efficiency solar steam generation to solve water resources scarcity.

1. Introduction

With the development of human society and increasing demand of fresh water for our daily lives, fresh-water shortage has become one of the most critical problems facing human society [1–3]. It is essential to find an efficient and environmentally friendly method to produce fresh-water [4–6] Solar steam generation, as an emerging water treatment technology [7,8], could produce fresh-water for water-scarce areas on the one hand, and on the other hand, makes full use of solar energy without harming the environment [9,10]. Hence solar steam generation

* Corresponding authors at: School of Energy and Power Engineering, Inner Mongolia University of Technology, Hohhot, Inner Mongolia 010051, China.
E-mail addresses: yxh1109@163.com (X. Yang), tianr@imut.edu.cn (R. Tian).

https://doi.org/10.1016/j.applthermaleng.2019.114379
Received 30 May 2019; Received in revised form 29 August 2019; Accepted 11 September 2019
Available online 20 September 2019
1359-4311/

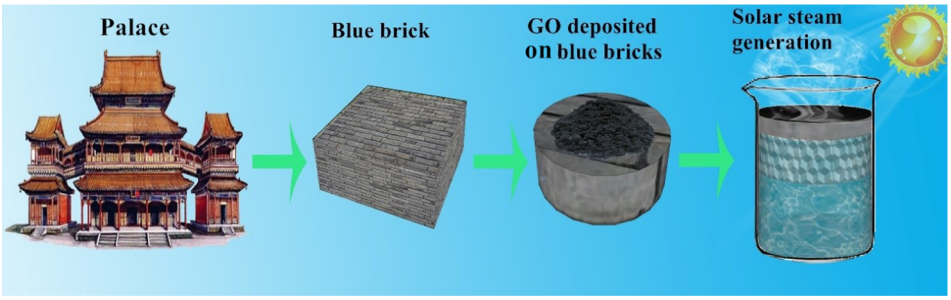

Fig. 1. Schematic diagram describing the structure of BBG and the manufacturing of solar steam generation device.

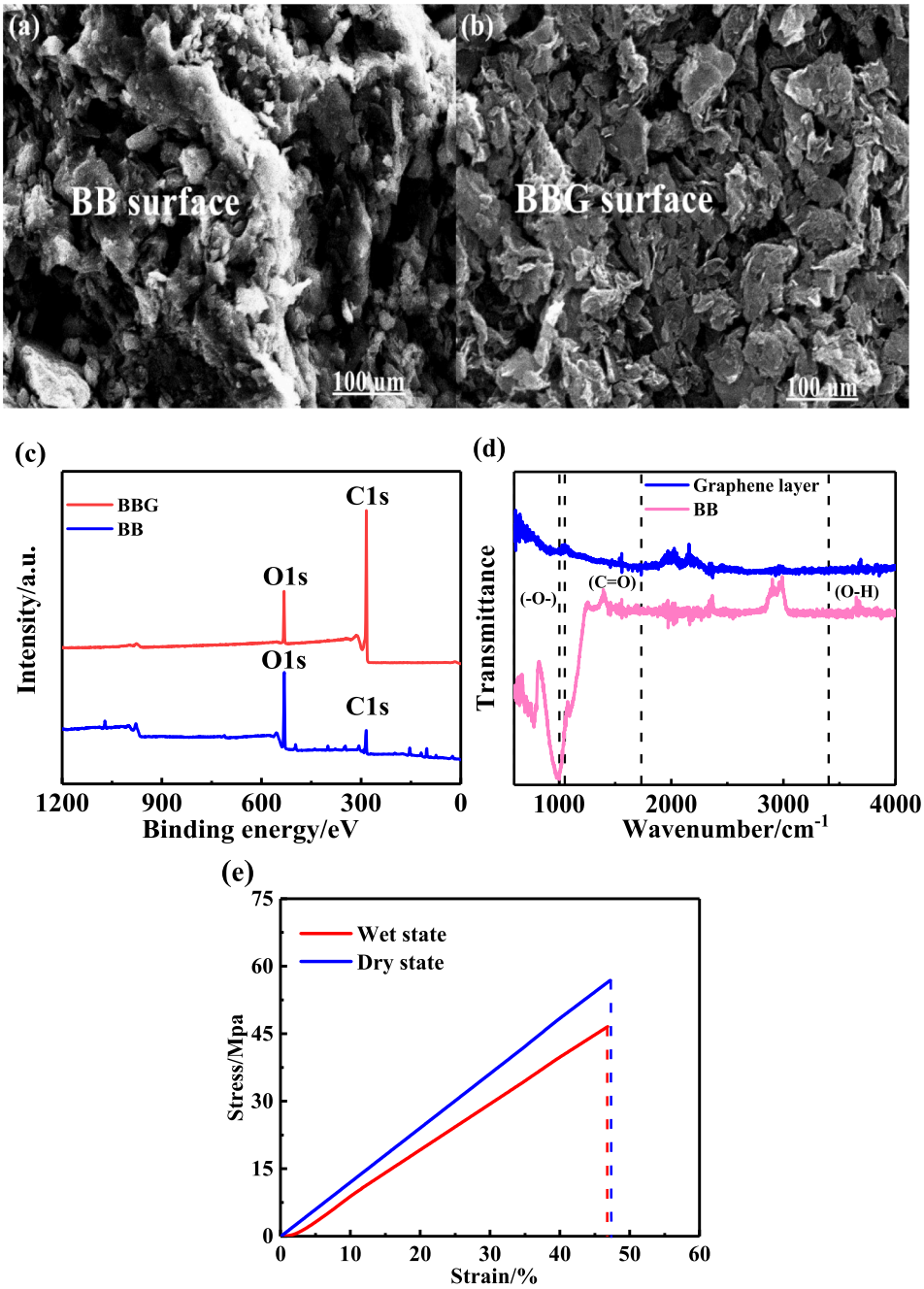

Fig. 2. Characterizations of BB and BBG: (a, b) SEM images of BB (a) and BBG (b) surface; (c) Wide-scan X-ray photoelectron spectroscopy (XPS) spectrum of BB and BBG; (d) Fourier transform infrared (FTIR) spectroscopy spectra of graphene and BB. (e) BB tensile strength in dry and wet states.

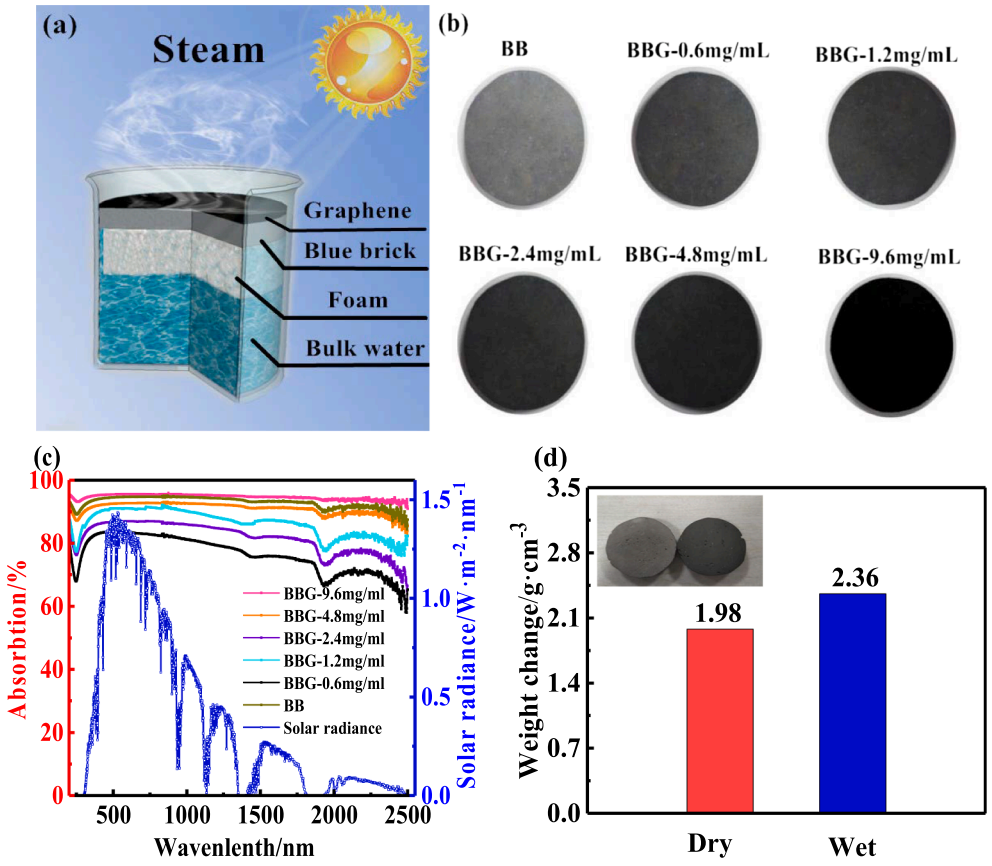

Fig. 3. Performance of the BBG system: (a) Structure diagram of BBG system; (b) The photograph of BB and BBGs with different graphene concentration; (c) Absorption spectra of BB and BBGs with different graphene concentration and solar spectral irradiance weighted by standard AM 1.5G solar spectrum; (d) The weight change between wet and dry of BB.

has been widely attracted by scholars in recent years.

A typical solar steam generation system should have efficient optical absorption capacity [11–13], good thermal management [14–16] and sufficient water supply capacity [17]. To improve the optical absorption efficiency [18,19] of evaporator, various light-absorbing materials [20,21], such as graphene [22–26], carbon black [27–28], aluminum nanoparticles and polypyrrole (PPy) [29] have been applied for light-heat conversion layer in recent years. In addition to light-heat conversion layer, thermal insulation layer is also important for improving evaporation performance of solar steam generation system. Some insulation materials, such as carbon foam [30], wood, aerogel, air-laid paper [31], and hydroxyapatite nanowires [32], have been used as thermal insulation layer to prevent heat losses to bulk water and supply water to light-heat conversion layer for evaporation.

At the same time, some structures have been designed by scientists to improve the evaporation performance. For example, based on the principles of bionics, natural mushroom was found to be efficient solar steam generation device by Zhu's group, and results showed that evaporation efficiency of carbonized mushroom could reach about 78% [33]. A flexible Janus absorber fabricated by sequential electrospinning was also demonstrated by Zhu et al., and results showed a high evaporation efficiency of about 72% [34]. Three-dimensional water evaporation based on a highly vertically ordered pillar array of graphene-assembled framework was reported by Qu's group, which exhibited satisfactory evaporation efficiency of about 95% [35]. More recently, Naik's group demonstrated introduced a novel bi-layered structure [36–40] composed of wood [41–43] and graphene oxide for a solar steam generation, and evaporation efficiency was calculated to be 82.8% at a power density of 12 suns (1 sun = 1 kW m^{-2}) [44]. In order to find a better thermal insulation layers, Hu et al. demonstrated that graphene oxide based on aerogels, thermal and hydrophilic [45] properties can enable evaporation efficiency about 83% solar steam generation [46]. Zhu's group [47] and Jiang's group [48] have reported 3D cone evaporators, and the evaporation efficiency can reach 85 and 93.8% respectively. Although these successful advances have been made in improving evaporation performance, the large-scale application of solar steam generation system is still limited by the complexity of material preparation process and high cost. It is essential to develop a low-cost and easy-to-process solar steam generation system which possesses efficient optical absorption property, sufficient water supply capacity and high evaporation efficiency.

In this work, a novel blue brick-graphene 3D inverted cone structure was designed for solar steam generation. The blue bricks (BBs) are made of inexpensive natural clay. BBs as a traditional building material with high evaporation performance has the following characteristics, such as suitable porosity, low thermal conductivity, excellent water supply capacity, high tensile strength, low-cost and easy-to-process. Blue brick-graphene which is called BBG for short is obtained by daubing graphene on the blue brick. It is found that BBG presents the characteristics of good heat management, light absorption, durability and desalination ability. The 9.6 mg/mL BBG who provides water for light-heat conversion layer from bulk water is very suitable as an excellent absorber for high efficiency. Meanwhile, the BBG 3D inverted cone reduces the contact area between the light absorption layer and water to suppress heat loss. And the air filling the cavity of inverted cone structure serves as an effective thermal barrier, which could effectively prevent the loss of heat to bulk water and ambient. Therefore, the temperature of the light absorption layer has been further increased. The optical absorption properties of BB and BBG 3D inverted cone were investigated and the optical absorption efficiency could reach about 76.4 and 97.3% respectively. As a result, the novel 3D inverted cone composite structure has a high evaporation efficiency of

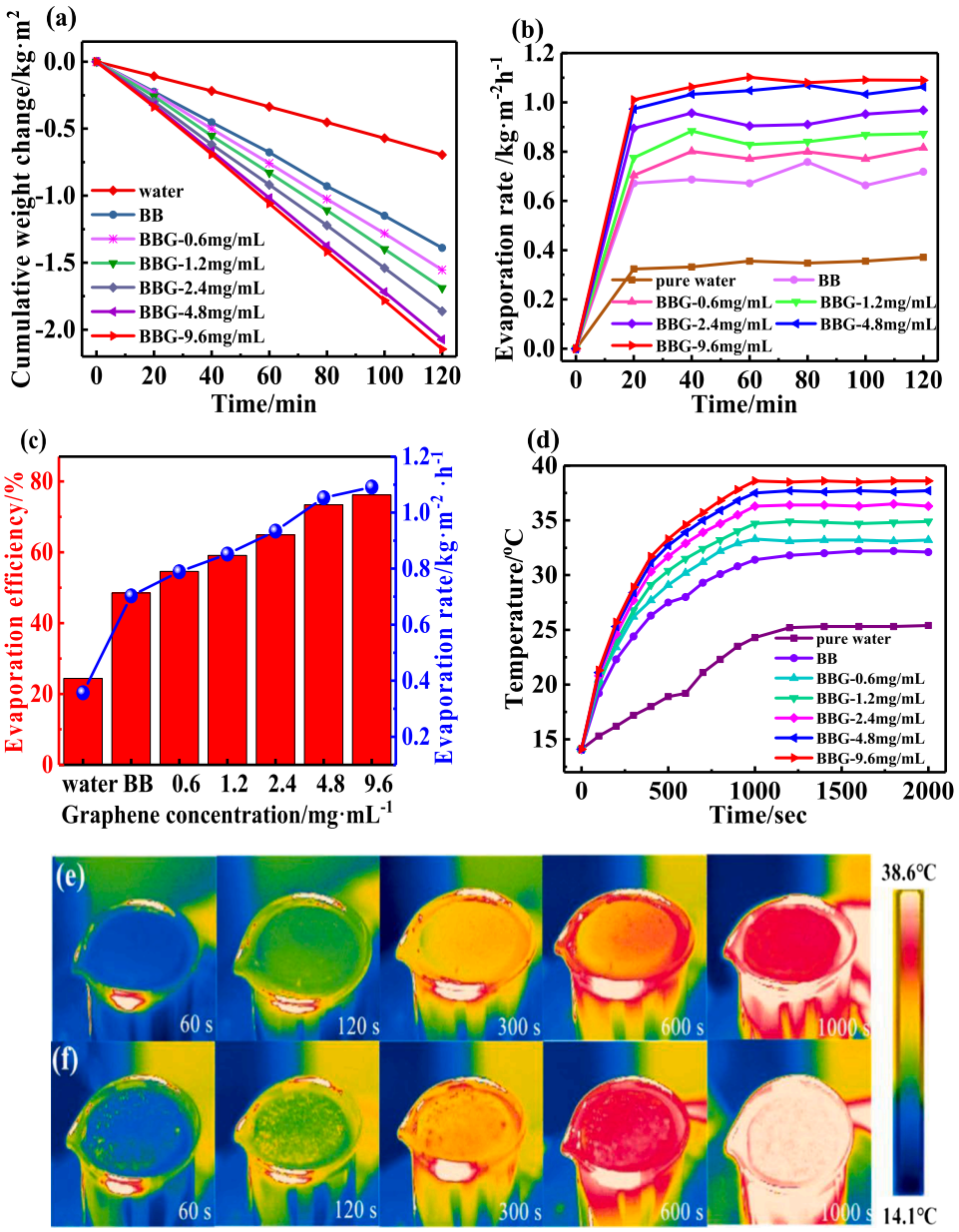

Fig. 4. Evaporation performance of BBGs systems: (a) The cumulative weight change of water; (b) The evaporation rate of the pure water, BB and BBGs with different concentration under one sun irradiation; (c) The relationship between evaporation efficiencies and evaporation rates of the pure water, BB and BBGs with different concentration; (d) The surface temperature versus irradiation time; (e, f) Temperature distributions in BB (e) and 0.96 mg/mL BBG (f) systems.

about 84% and excellent water purification capacity. This work can provide a new method for high-efficiency solar steam generation to solve water resources scarcity.

2. Fabrication and characterization of BBG

2.1. Fabrication of BBG

In this work, graphene was synthesized by microwave method reported by a patent of partner company [49]. Firstly, the graphite was placed in a microwave expansion device for rapid expansion to obtain worm-like graphite. Secondly, the worm-like graphite was subjected to an oxidation reaction, and the dried graphite oxide was obtained after washing and drying. Subsequently, the dried graphite oxide was placed into a microwave reduction device for vacuum stripping. Finally, dried graphene powders were obtained by reduction under inert gas protection. The thermal conductivities of graphene powder were about 4864 W m^{-1} K^{-1} by a thermal constants analyser.

Owing to abundance of clay in nature, BB was made from natural clay by flame treatment as exhibited in Fig. 1. BB, as a building material for thousands of years, has hydrophilicity, excellent thermal insulation, stand wear, which was a good candidate as the thermal insulation layer.

The BBG composite was fabricated by deposition method. Firstly, BB taken from ancient construction waste were cut into thin slices with a diameter of 35 mm and a thickness of 3 mm, then dried naturally to remove internal moisture. Subsequently, the prepared graphene was dissolved in deionized water, and then stirred for 40 min with an ultrasonic cell crusher. Finally, the BBG composite evaporator was obtained by daubing graphene solution uniformly on blue brick and dried naturally. The polystyrene foam provides buoyancy to the BBG composite so that it can float on the water surface.

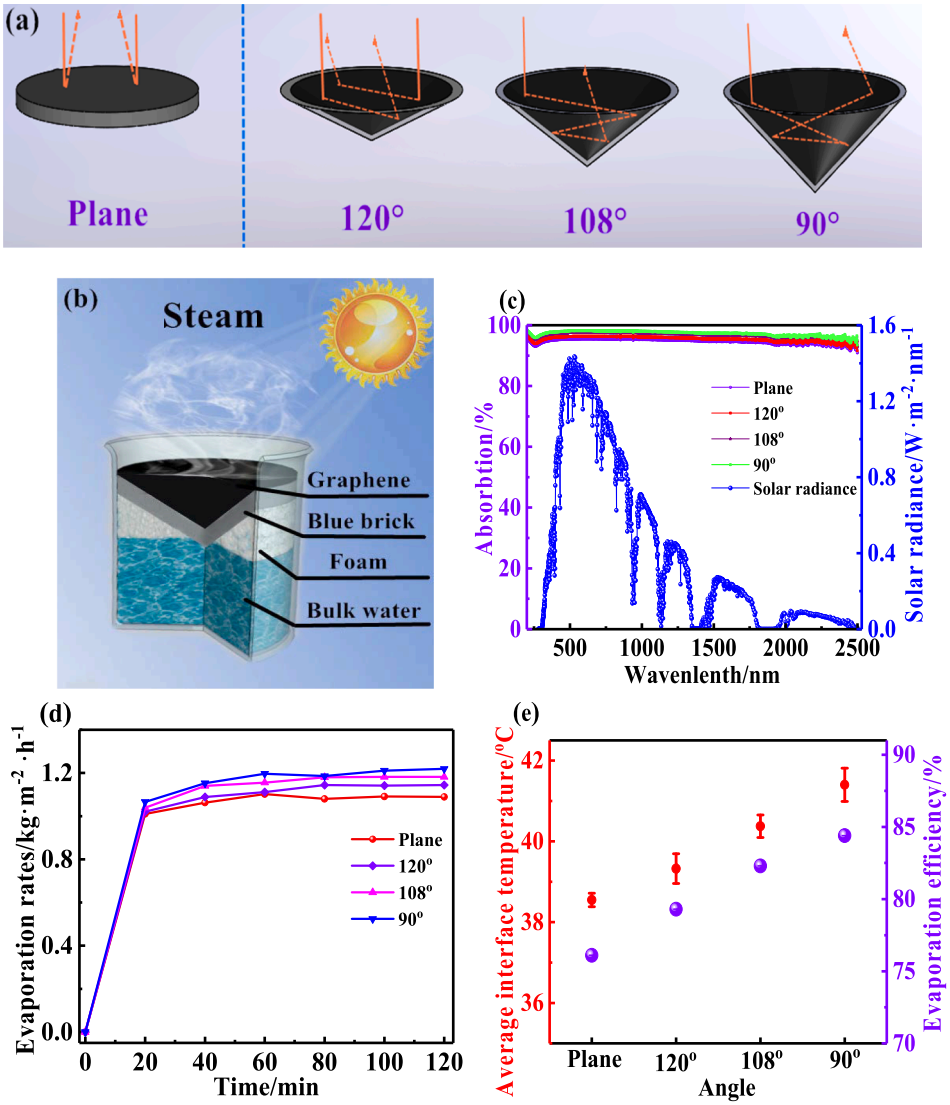

Fig. 5. Evaporation performance of BBG inverted cones. (a) Schematic diagram of BBG inverted cones are shown with different apex angle; (b) Structure diagram of BBG inverted cones; (c) Absorption spectra of BBG inverted cones; (d) The evaporation rate of the BBG inverted cones; (e) The relationship between average interface temperature and evaporation efficiency of BBG inverted cones.

2.2. Evaporation property calculation

For solar steam generation, the evaporation rate ($\dot{m}$) can be calculated by,

$$\dot{m} = \frac{\Delta m}{A \cdot t} \tag{1}$$

where $\dot{m}$ is the evaporation rate ($kg\,m^{-2}\,h^{-1}$), A is the evaporation area (m^2), Δm is weight change of water (kg), and t is the irradiation time (h). The evaporation efficiency (η) is defined as the ratio of the heat absorbed by water during evaporation to the total incident energy to the BBG,

$$\eta = \frac{\dot{m} h_{LV}}{I} \tag{2}$$

where h_{LV} is the total enthalpy change of liquid-vapor phase change, which is the sum of phase-change enthalpy ($2410\,kJ\,kg^{-1}$ in this work) and sensible heat, where the specific heat capacity of water is about $4.2\,kJ\,kg^{-1}\,K^{-1}$. I is the solar radiation heat flux density ($1\,kW\,m^{-2}$ in this work).

Porosity is an important parameter affecting water supply and effective thermal conductivity performance of BB, the porosity of BB is defined as,

$$\varepsilon = \frac{m_2 - m_1}{V \rho_w} \tag{3}$$

where m_2 is the weight of BB in a completely wet state, $m_1$is the weight of BB in dry state, is the volume of the sample BB, here a sample with a volume of $1\,cm^3$ was took for testing. $\rho_w$is the density of water, i.e. $1\,g\,cm^{-3}$.

2.3. Characterization

The light absorption of BB and BBG were measured by UV-3600 spectrometer (Shimadzu, Japan). The surface microstructures were detected by a Hitachi SU-3400 field emission scanning electron microscope (SEM). The X-ray photoelectron spectroscopy (XPS, Thermo ESCALAB 250Xi) was used to detect surface chemical elements. The Fourier transform infrared spectroscopy (FT-IR) spectra were measured by a Thermo Nicolet NEXUS 870 FTIR. The absorption surface temperature distribution of the device was obtained by an infrared thermal camera (FLIR T200 Infrared Camera). The water temperature changes of pure water, BB and BBG were tested by k-type thermocouple. The ion concentrations were measured by high resolution inductively coupled

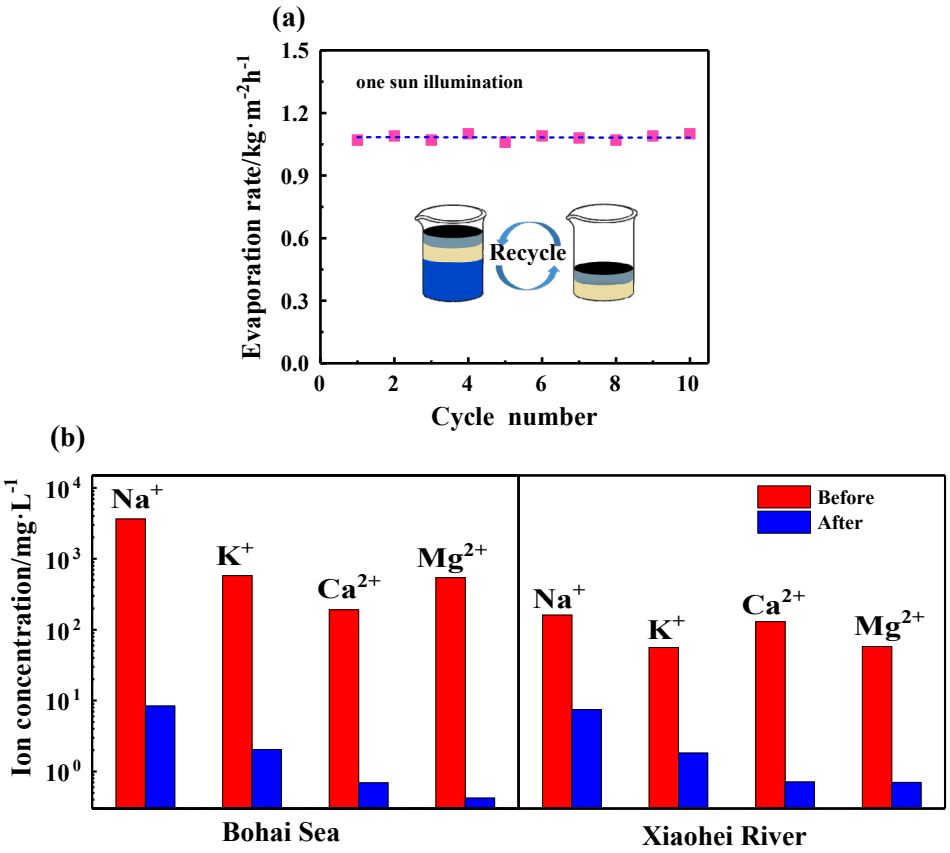

Fig. 6. Durability and desalination ability and of BBGs. (a) Cycling performance of BBGs; (b) Four primary ions concentrations of the actual seawater (Bohai Sea) and river water (Xiaohei River) were measured before and after desalination.

plasma mass spectroscopy (HRICP-MS, ELEMENT2 USA). Incident light source was provided by the TRM-PD artificial solar simulator (TRM-PD China). The incident power density was measured by TBQ-2 series solar pyranometer (TBQ-2 China). The thermal conductivity was measured by a thermal constants analyser (Hot Disk TPS 2500, China). The ambient temperature and humidity were about 15 °C and 20% respectively.

3. Results and discussion

3.1. Characterizations of BBG

The surface microstructures of BB and BBG were observed by SEM. As illustrated in Fig. 2a, the surface of BB exhibited the porous microstructure, which could provide channels for the rapid infiltrated through a sufficient supply of water. The black graphene layer could be clearly observed in Fig. 2b, graphene was evenly distributed on BB surface. However, BBG has rough surface and porous microstructure, which reduces the loss of incident light and enhances the ability of light acquisition. For the graphene layer, unobstructed water penetration through nanoscale pores could be used as a water filter. The surface chemical compositions and functional groups of BB and BBG were detected by XPS and FTIR respectively. Fig. 2c shows XPS spectra of BB and BBG, two apparent peaks were detected at ~555.08 eV and ~284.08 eV, corresponding to O 1s and C 1s signals respectively. Therefore, the result also confirms the chemical elements on surface of BB and BBG evaporators. In addition, Fig. 2d presented FTIR spectra of BB and BBG, the tiny band at 1733 cm^{-1} were tested to be carbonyl group. The band at 1051 cm^{-1} were tested to be −O− groups, and the tiny band at 3403 cm^{-1} attributed to OH stretching. The OH and C═O groups indicated the excellent hydrophilicity of BB and BBG. In addition, dynamic contact angles of BB and BBG were demonstrated in Figs. S2 and S3, further confirming excellent hydrophilicity. It can be seen that BB have high tensile strength of 56.8 and 46.5 MPa in the dry and wet state respectively could be processed and applied.

3.2. Effect of graphene concentration

The experimental structure of our work was illustrated in Fig. 3a. BBG was placed on the foam to ensure that it could float on water surface. The foam can provide a properly buoyancy to make the BBG contacted with bulk water surface. The optical images of BB and BBGs with different graphene concentration were exhibited in Fig. 3b. The color of BBGs were obviously darker than the previous one, because BBGs were obtained by increasing the concentration of graphene on BB surface. Solar energy is the energy source of the system, and the high absorption efficiency is a guarantee for energy conversion of solar steam generation system. In order to determine the optical absorption efficiency of evaporator, broadband light absorption of BB and BBGs were detected under AM 1.5 G solar spectral irradiance. As exhibited in Fig. 3c, With the increase of graphene concentration from 0 to 9.6 mg/mL, the optical absorption performance increase rapidly. The optical absorption efficiency of 9.6 mg/mL BBG could reach about 94.7%, while that of BB was only 76.4%. Consequently, solar energy can be effectively collected by 9.6 mg/mL BBG system.

In addition, the average weight of our samples with the volume of 1 cm^3 were tested in wet and dry state in Fig. 3d, and the density was calculated to be about 1.98 g cm^{-3}. The porosity of BB is approximately 38% based on Eq. (3), which ensures that the heat loss could be controlled at a lower value. The thermal conductivity is a crucial factor affecting heat conduction to bulk water, further influencing evaporation performance. In addition, the thermal conductivities of BB under

dry and wet state were 0.526 and 1.080 $W m^{-1} K^{-1}$ respectively. It can be seen that BB has excellent thermal insulation ability, which could be applied as thermal insulation material for solar steam generation.

To evaluate the performance of BB and BBGs as the solar steam generation devices. The evaporation rate and efficiency were measured by cumulative weight change of water. Firstly, the evaporation rates of BB and 9.6 mg/mL BBG system were 0.024 and 0.033 $kg m^{-2} h^{-1}$ in the dark field respectively, while the evaporation rate of pure water was only 0.017 $kg m^{-2} h^{-1}$ in Fig. S3. The increase in evaporation rate was attributed to the large specific surface area of BB and BBGs. At the same time, the surface temperature distribution of BB and BBGs were slightly lower than the one of pure water in the dark field, further confirm that BB and BBGs were more benefit for steam escape. Secondly, under one sun irradiation, stable evaporations of BB and BBGs were achieved through the excellent structure as exhibited in Fig. 4a–b. Obviously, the cumulative weight change of water gradually decreases versus irradiation time in the experiment. And the cumulative weight change of water was gradually increasing with the increase of graphene concentration from 0 to 9.6 mg/mL. At this time, increase the graphene concentration, the weight change is no longer apparent. After 20 min of stable irradiation, the evaporation rates of BB and 9.6 mg/mL BBG were calculated to be about 0.70 and 1.09 $kg m^{-2} h^{-1}$ respectively, which were 1.9 and 3.0 times than the one of pure water (0.36 $kg m^{-2} h^{-1}$). According to the Eq. (2), the evaporation efficiency of pure water and BB is only 24.4% and 48.5% respectively, and BBGs can reach 76.2% with the increase of concentration as shown in Fig. 4c. Therefore, 9.6 mg/mL BBG could be used as an excellent light absorber for high efficiency solar steam generation.

To confirm heat localization capacity of BBGs, temperature changes of pure water, BB and 9.6 mg/mL BBG were measured by k-type thermocouple and the IR images were exhibited in Fig. 4d–f. The surface temperature of 9.6 mg/mL BBG could increase from about 14.1 °C to 38.6 °C. Meanwhile, the surface temperature of BB could reach about 32.2 °C, while that of pure water could only reach about 25.3 °C under the same conditions. The surface temperature distributions of BB and 9.6 mg/mL BBG were photographed at difference time as illustrated in Fig. 4f. At the beginning, the surface temperature of the BB and BBG increased rapidly, and then tends to a constant value after about 1000 s. As mentioned previously, the 9.6 mg/mL BBG possess an excellent evaporation performance and stable heat localization.

3.3. Evaporation performance enhanced by inverted cone structure

As illustrated in Fig. 5a, in order to retain more light energy and generate more steam on a limited area, this work provides a novel BBG inverted cone structure for efficient light energy harvesting. The diffuse reflection of light can control the absorption of light. At the same graphene concentration of 9.6 mg/mL, the 2D plane structure and 3D inverted cone structure with different apex angles of the vertical incident light source were demonstrated. Compared with the plane structure, incident light will be reflected and absorbed multiple times inside the vertebral body, which weakens the loss of light energy. And at this time the evaporation area and the radiation area refer to the side areas of the inverted cone structure. However, with the decrease of the apex angle of the evaporator, the reflection and absorption of incident light become more intense. Therefor leading the light absorption efficiency is gradually improved with the reduction of the apex angle of the inverted cone. When the apex angle is 90° 3D inverted cone, the light absorption rate can reach 97.3% in Fig. 5c, further verified that light can be better absorbed after diffuse reflection in the inverted cone structure.

As show in Fig. 5b, based on the inverted cone structure, the design of the bottom apex angle area of the inverted cone contact with the bulk water surface and reduces the contact area between the water and the evaporator. When the apex angle of the evaporator contacts water, water can quickly infiltrate the whole vertebral body through its own efficient water transport.

Because 3D inverted cones reduce the contact area between the light absorption layer and water, and prevents the loss of heat to bulk water. And the air filling the cavity of inverted cone structure serves as an effective thermal barrier to suppress heat loss. Therefore, the surface temperature increases with the apex angle decreases and further improve the evaporation performance of BBG. Based on the inverted cone structure, the evaporation rate is about 0.033 $kg m^{-2} h^{-1}$, which approximates the same concentration of the plane structure and other angles inverted cone structure in Fig. S3. The evaporation rates of 120° 3D inverted cone can be stabilized at 1.14 $kg m^{-2} h^{-1}$ after 20 min in Fig. 5d, which higher than the 2D plane structure under one sun illumination. As the apex angle decreases, the evaporation rates of 90° 3D inverted cone attach 1.21 $kg m^{-2} h^{-1}$. Under the same illumination conditions, smaller heat loss of 3D inverted cone structure increases evaporation temperature and accelerates the escape of steam. Due to the complexity of BBG process, it would be an ideal absorber if it was fabricated as a honeycomb-like multi-groove structure.

As illustrated in Fig. 5e. The temperature of optical absorption layer of 90° inverted cone can reach 41.5 °C. According to the Eq. (2), the evaporation efficiency of 120° 3D inverted cone and 108° 3D inverted cone were 79.2% and 82% respectively. The evaporation efficiency gradually increases as the apex angle decrease, 90° 3D inverted cone reach up to 84.0% evaporation efficiency. The results show intelligent 3D inverted cone structure is an ideal absorber for efficiency solar steam generation.

3.4. Durability and desalination ability of BBG

The cycle performance of BBG systems were also tested under one sun irradiation as exhibited in Fig. 6a. Results show that a stable performance of BBG systems were confirmed through 10 cycles with each being over one hour. After the experiment, dilute acetic acid was added to the surface of BBG to remove the salt crystals, which were appeared on BBG surface thanks to vapor escaped in Fig. S6, and the evaporation performance was particularly stable after multiple cycles. It shows that BBG has good durability and could be used for long-term desalination. In addition, the seawater samples from the Bohai Sea and Xiaohei River were applied for desalination. As show in Fig. 6b, all four primary ions concentrations (Mg^{2+}, Na^{+}, Ca^{2+} and K^{+}) after purification were significantly reduced, and the ion rejection ratios of four primary ions were close to 99.8% of a seawater sample. The collected condensate water meets the World Health Organization (WHO) drinking water requirements.

4. Conclusion

In summary, a bi-layered inverted cone structure is prepared by daubing graphene on blue brick, which presents the characteristics of low thermal conductivity, excellent water supply capacity and high optical absorption property. Under one sun stable irradiation, 9.6 mg/mL as a suitable concentration, the evaporation rate and efficiency of plane structure can be about 1.09 $kg m^{-2} h^{-1}$ and 76.2%. Based on the inverted cone structure, enhanced light absorption, reduced heat loss, increased surface temperature and improved steam performance. So, the optical absorption efficiency could reach about 97.3%, and the high evaporation rate and efficiency of about 1.21 $kg m^{-2} h^{-1}$ and 84%. In addition, the BBG shows an excellent water purification capacity for long-term recycling, all four primary ions concentrations after purification are significantly reduced and the ion rejection ratios of four primary ions are close to 99.8%. Hence, we conclude that this work could provide a new method for high-efficiency solar steam generation to solve water resources scarcity.

Acknowledgements

This work has been supported by the National Natural Science Foundation of China (51866011) and Inner Mongolia Natural Science Foundation of China (2017MS(LH)0504), we also acknowledge the support for graphene product preparation from the Qingdao International Graphene Innovation Center.

Appendix A. Supplementary material

Supplementary data to this article can be found online at https://doi.org/10.1016/j.applthermaleng.2019.114379.

References

[1] Y. Yang, R. Zhao, T. Zhang, K. Zhao, P. Xiao, Y. Ma, Y. Chen, Graphene-based standalone solar energy converter for water desalination and purification, ACS Nano 12 (2018) 829–835.
[2] E.D. Miao, M.Q. Ye, C.L. Guo, L. Liang, Q. Liu, Z.H. Rao, Enhanced solar steam generation using carbon nanotube membrane distillation device with heatlocalization, Appl. Therm. Eng. 149 (2019) 1255–1264.
[3] O. Neumann, A.S. Urban, J. Day, S. Lal, P. Nordlander, N.J. Halas, Solar vapor generation enabled by nanoparticles, ACS Nano 7 (2013) 42–49.
[4] H. Sharon, K.S. Reddy, A review of solar energy driven desalination technologies, Renew. Energy Rev 41 (2015) 1080–1118.
[5] M.M. Gao, L. Zhu, C.K. Peh, G.W. Ho, Solar absorber material and system designs for photothermal water vaporization towards clean water and energy production, Energy Environ. Sci. 12 (2019) 841–864.
[6] Masahiro Fujiwara, Water desalination using visible light by disperse red 1 modified PTFE membrane, Desalination 404 (2017) 79–86.
[7] M.M. Gao, C.K. Peh, H.T.L. Phan, L. Zhu, G.W. Ho, Solar absorber gel: localized macro-nano heat channeling for efficient plasmonic Au nanoflowers photothermic vaporization and triboelectric generation, Adv. Energy Mater. 8 (2018) 1800711.
[8] S. Liu, C.L. Huang, X. Luo, Z.H. Rao, Performance optimization of bi-layer solar steam generation system through tuning porosity of bottom layer, Appl. Energy 239 (2019) 504–513.
[9] M.Q. Yang, M.M. Gao, M.H. Hong, G.W. Ho, Visible-to-NIR photon harvesting: progressive engineering of catalysts for solar-powered environmental purification and fuel production, Adv. Mater. 30 (2018) 1802894.
[10] S. Homaeigohar, M. Elbahri, Graphene membranes for water desalination, NPG Asia Mater. 9 (2017) e427.
[11] X. Wang, Y. He, X. Liu, G. Cheng, J.Q. Zhu, Solar steam generation through bio-inspired interface heating of broadband-absorbing plasmonic membranes, Appl. Energy 195 (2017) 414–425.
[12] H.S. Wang, M.K. Liu, H. Kong, Y. Hao, Thermodynamic analysis on mid/low temperature solar methane steam reforming with hydrogen permeation membrane reactors, Appl. Therm. Eng. 152 (2019) 925–936.
[13] J. Xu, F. Xu, M. Qian, Z. Li, P. Sun, Z. Hong, F. Huang, Copper nanodot-embedded graphene urchins of nearly full-spectrum solar absorption and extraordinary solar desalination, Nano Energy 53 (2018) 425–431.
[14] Y. Ito, Y. Tanabe, J. Han, T. Fujita, K. Tanigaki, M. Chen, Multifunctional porous graphene for high-efficiency steam generation by heat localization, Adv. Mater. 27 (2015) 4302–4307.
[15] H. Ghasemi, G. Ni, A.M. Marconnet, J. Loomis, S. Yerci, N. Miljkovic, G. Chen, Solar steam generation by heat localization, Nat. Commun. 5 (2014) 4449.
[16] J. Lou, Y. Liu, Z. Wang, D. Zhao, C. Song, J. Wu, N. Dasgupta, W. Zhang, D. Zhang, P. Tao, W. Shang, T. Deng, Bioinspired multifunctional paper-based RGO composites for solar-driven clean water generation, ACS Appl. Mater. Interfaces 8 (2016) 14628–14636.
[17] L. Zhou, Y. Tan, J. Wang, W. Xu, Y. Yuan, W. Cai, S. Zhu, J. Zhu, 3D self-assembly of aluminium nanoparticles for plasmon-enhanced solar desalination, Nature Photon 10 (2016) 393–398.
[18] F. Wang, D.Y. Wei, Y.Z. Li, T. Chen, P. Mu, H.X. Sun, Z.Q. Zhu, W.D. Liang, A. Li, Chitosan/reduced graphene oxide-modified spacer fabric as a salt-resistant solar absorber for efficient solar steam generation, J. Mater. Chem. A 7 (2019) 18311–18317.
[19] L.L. Zhu, T.P. Ding, M.M. Gao, C.K. Peh, G.W. Ho, Shape conformal and thermal insulative organic solar absorber sponge for photothermal water evaporation and thermoelectric power generation, Adv. Energy Mater. 9 (2019) 1900250.
[20] F. Zhao, X. Zhou, Y. Shi, X. Qian, M. Alexander, X. Zhao, S. Mendez, R. Yang, L. Qu, G. Yu, Highly efficient solar vapour generation via hierarchically nanostructured gels, Nat. Nanotechnol. 13 (2018) 489–495.
[21] E. Garnett, P. Yang, Light trapping in silicon nanowire solar cells, Nano Lett. 10 (2010) 1082–1087.
[22] D.H. Seo, S. Pineda, Y.C. Woo, M. Xie, A.T. Murdock, E.Y.M. Ang, K.K. Ostrikov, Anti-fouling graphene-based membranes for effective water desalination, Nat. Commun. 9 (2018) 683.
[23] D. Cohen-Tanugi, L.C. Lin, J.C. Grossman, Multilayer nanoporous graphene membranes for water desalination, Nano Lett. 2 (2016) 1027–1033.
[24] K. Bae, G. Kang, S.K. Cho, W. Park, K. Kim, W.J. Padilla, Flexible thin-film black gold membranes with ultrabroadband plasmonic nanofocusing for efficient solar vapour generation, Nat. Commun. 6 (2015) 10103.
[25] G.P. Liu, W.Q. Jin, Graphene oxide membrane for molecular separation: challenges and opportunities, Sci. China Mater. 61 (2018) 1021–1026.
[26] H. Ren, M. Tang, B. Guan, K. Wang, J. Yang, F. Wang, M. Wang, J. Shan, Z. Chen, D. Wei, H. Peng, Z. Liu, Hierarchical graphene foam for efficient omnidirectional solar-Thermal energy conversion, Adv. Mater. 8 (2017) 1702590.
[27] S. Liu, C. Huang, X. Luo, Z. Rao, High-performance solar steam seneration of a paper-based carbon particle system, Appl. Therm. Eng. 142 (2018) 566–572.
[28] Z. Yin, H. Wang, M. Jian, Y. Li, K.L. Xia, M.C. Zhang, C.Y. Wang, Q. Wang, M. Ma, Q. Zheng, Y. Zhang, Extremely black vertically-aligned carbon nanotube arrays for solar steam generation, ACS Appl. Mater. Interfaces 9 (2017) 28596–28603.
[29] L. Zhou, Y. Tan, J. Wang, W. Xu, Y. Yuan, W. Cai, J. Zhu, 3D self-assembly of aluminium nanoparticles for plasmon-enhanced solar desalination, Nat. Photon. 10 (2016) 393–398.
[30] L. Zhu, M. Gao, C.K.N. Peh, X. Wang, G. Ho, Self-contained monolithic carbon sponges for solar-driven interfacial water evaporation distillation and electricity generation, Adv. Energy Mater. 8 (2018) 1702149.
[31] G. Wang, Y. Fu, X. Ma, W. Pi, D. Liu, X. Wang, Reusable reduced graphene oxide based double-layer system modified by polyethylenimine for solar steam generation, Carbon 114 (2017) 117–124.
[32] Z. Xiong, Y. Zhu, D. Qin, F. Chen, R. Yang, Flexible fire-resistant photothermal paper comprising ultralong hydroxyapatite nanowires and carbon nanotubes for solar energy-driven water purification, Small 14 (2018) 1803387.
[33] N. Xu, X. Hu, W. Xu, X. Li, L. Zhou, S. Zhu, J. Zhu, Mushrooms as efficient solar steam-generation devices, Adv. Mater. 29 (2017) 1606762.
[34] W. Xu, X. Hu, S. Zhuang, Y. Wang, X. Li, L. Zhou, J. Zhu, Flexible and salt resistant janus absorbers by electrospinning for stable and efficient solar desalination, Adv. Energy Mater. 8 (2018) 1702884.
[35] P. Zhang, Q. Liao, H. Yao, H. Cheng, Y. Huang, C. Yang, L. Jiang, L. Qu, Three-dimensional water evaporation on a macroporous vertically aligned graphene pillar array under one sun, J. Mater. Chem. A 6 (2018) 15303.
[36] Y. Li, T. Gao, Z. Yang, C. Chen, Y. Kuang, J. Song, C. Jia, Emily M. Hitz, B. Yang, L. Hu, Graphene oxide-based evaporator with one-dimensional water transport enabling high-efficiency solar desalination, Nano Energy 41 (2017) 201–209.
[37] X. Li, W. Xu, M. Tang, L. Zhou, B. Zhu, S. Zhu, J. Zhu, Graphene oxide-based efficient and scalable solar desalination under one sun with a confined 2D water path, Pro. Nat. Acad. Sci. 113 (2016) 1613031.
[38] Y. Yang, H. Zhao, Z. Yin, J. Zhao, X. Yin, N. Li, D. Yin, Y. Li, B. Lei, Y. Du, W. Que, A general salt-resistant hydrophilic/hydrophobic nanoporous double layer design for efficient and stable solar water evaporation distillation, Mater. Horiz. 5 (2018) 1143–1150.
[39] S. Liu, C.L. Huang, Q. Huang, F.C. Wang, C.W. Guo, A new carbon-black/cellulose-sponge system with water supplied by injection for enhancing solar vapor generation, J. Mater. Chem. A 7 (2019) 17954–17965.
[40] Y. Liu, S. Yu, R. Feng, A. Bernard, Y. Liu, Y. Zhang, H. Duan, W. Shang, P. Tao, C. Song, T. Deng, A bioinspired, reusable, paper-based system for high-performance large-scale evaporation, Adv. Mater. 27 (2015) 2768–2774.
[41] Q.S. Jiang, S. Singamaneni, Water from wood: pouring through pores, Joule 3 (2017) 429–430.
[42] B. Feng, K. Xu, A. Huang, Covalent synthesis of three-dimensional graphene oxide framework (GOF) membrane for seawater desalination, Desalination 394 (2016) 123–130.
[43] L.L. Zhu, M. Gao, C.K. Peh, G.W. Ho, Recent progress in solar-driven interfacial water evaporation: Advanced designs and applications, Nano Energy 57 (2018) 507–518.
[44] K.K. Liu, Q. Jiang, S. Tadepalli, R. Raliya, P. Biswas, R.R. Naik, S. Singamaneni, Wood-graphene oxide composite for highly efficient solar steam generation and desalination, ACS Appl. Mater. Interfaces 9 (2017) 7675–7681.
[45] L. Feng, H.Y. Liao, P. Wang, J. Huang, K.L. Schumacher, A technique to avoid two-phase flow in solar collector tubes of the direct steam generation system for asolar aided power generation plant, Appl. Therm. Eng. 148 (2019) 568–577.
[46] X. Hu, W. Xu, L. Zhou, Y. Tan, Y. Wang, S. Zhu, Tailoring graphene oxide-based aerogels for efficient solar steam generation under one sun, Adv. Mater. 29 (2016) 1604031.
[47] X.Q. Li, R.X. Lin, G. Ni, N. Xu, X.Z. Hu, B. Zhu, G.X. Lv, J.L. Li, S.N. Zhu, J. Zhu, Three-dimensional artificial transpiration for efficient solar waste-water treatment, Natl. Sci. Rev. 5 (2018) 70–77.
[48] Y.C. Wang, C.Z. Wang, X.J. Song, M.H. Huang, S.K. Megarajan, S.F. Shaukat, H.Q. Jiang, Improved light-harvesting and thermal management for efficient solar-driven water evaporation using 3D photothermal cones, J. Mater. Chem. A 6 (2018) 9749–10152.
[49] G. Feng, N. Qiu, X.Z. Wang, A microwave-assisted method for the production of graphene, CN201510658686.8, 2016.